International Journal of GEOMATE, Aug., 2018 Vol.15, Issue 48, pp.10-15
Geotec., Const. Mat. & Env., DOI: https://doi.org/10.21660/2018.48.7320
ISSN: 2186-2982 (Print), 2186-2990 (Online), Japan

LIQUEFACTION SIMULATION AND RELATED BEHAVIOR OF UNDERGROUND STRUCTURE ON OSAKA GULF COAST

*Keita Sugito[1], Tetsuya Okano[2] and Ryoichi Fukagawa[3]

[1,2]Graduate School of Science and Engineering, Ritsumeikan University, Japan; [3]Department of Science and Engineering, Ritsumeikan University, Japan

*Corresponding Author, Received: 10 June 2017, Revised: 07 Aug. 2017, Accepted: 10 Sept. 2017

ABSTRACT: The Kansai area has a high possibility of a huge plate-boundary-type earthquake within 30 years. If an earthquake occurs, the Osaka Gulf coast will be struck by severe liquefaction disasters. Therefore, we tried to apply LIQCA, which is often used for liquefaction analysis, to a site on the Osaka Gulf coast. The input earthquake motion is the seismic standard spectrum I, which is commonly used in Japan. The calculation time continued until the excess pore water pressure dissipated. The site has an underground structure, so we investigated not only the liquefaction phenomenon of the ground itself but also the behavior of the underground structure. The results of this analysis indicate that these soil layers of the target area become liquefied. After the excess pore water pressure dissipates, the ground surface settles in the vertical direction and moves in the horizontal direction. In addition, in the vicinity of the underground structure center, it rises in the vertical direction and moves in the horizontal direction.

Keywords: Liquefaction, Numerical simulation, Tunnel, Float up

1. INTRODUCTION

A Nankai trough earthquake, which is a plate-boundary-type huge earthquake, has a high probability of occurring within 30 years, and the western part of Japan will be severely damaged by this earthquake. The Osaka Plain is no exception. In particular, the Osaka Gulf coast is predicted to suffer from a severe liquefaction disaster [1]. Therefore, we apply a liquefaction simulation to a typical site on the Osaka Gulf coast. The simulation is based on the LIQCA [2] program, which is widely used as a liquefaction simulation tool in Japan. As liquefaction occurs in the target ground, grasp the parts that are greatly damaged. The target ground has a tunnel beneath the ground, so we investigated not only the liquefaction phenomenon of the ground itself but also the behavior of the underground structure.

2. OUTLINE OF ANALYSIS

2.1 Ground to be analyzed

The analysis target is the ground of a plain on the Osaka Gulf coast. Fig. 1 shows the cross-section of the ground that is the target of the analysis. The cross-section has a length of 100 m in the horizontal direction and a depth of 40 m in the vertical direction. The tunnel that trains pass through is located near the surface in the center of the ground. The names of the ground are B layer, Ac1 layer, As1 layer, Ac2 layer, As2 layer, Tsg1 layer, Tc1 layer, Tsg2 layer, Tc2 layer, Oc layer in order from the closest to the ground surface. The soil layers that may liquefy are the As1 layer, As2 layer, and Tsg1 layer. Other layers are composed of clayey soil and hard, sandy soil. Thus, it is considered that liquefaction barely occurs. Therefore, these layers are not judged for liquefaction.

The groundwater level is set at GL-2.3 m. The Oc layer is the base surface in this cross-section. In the B layer, the layer above the groundwater level is considered hard to liquefy, so the R-O model is applied to this layer. The layer below the groundwater level is modeled as a cyclic elastoplastic constitutive model. Table 1 lists the material parameters used in the analysis. The liquefaction layers and non-liquefaction layers are fitted based on the respective standards. The liquefaction layers have liquefaction strength curves based on the *Design Standards for Railway Structures and Commentary* [3]. Shear modulus and shear strain relation (G/G_{max}~ γ), history attenuation and shear strain relation (h~γ) were referenced using element simulation. These were used to determine the nonlinear properties of the non-liquefaction layer. Since G/G_{max}~γ and h~γ relationship are different for each soil, it is also highly dependent on constraint pressure, it is preferable to calculate by an indoor test such as a repeated triaxial test of specimen sampled from the ground. A past empirical formula was used in this analysis. The non-liquefaction layers are fitted as a Yasuda-Yamaguchi model [4].

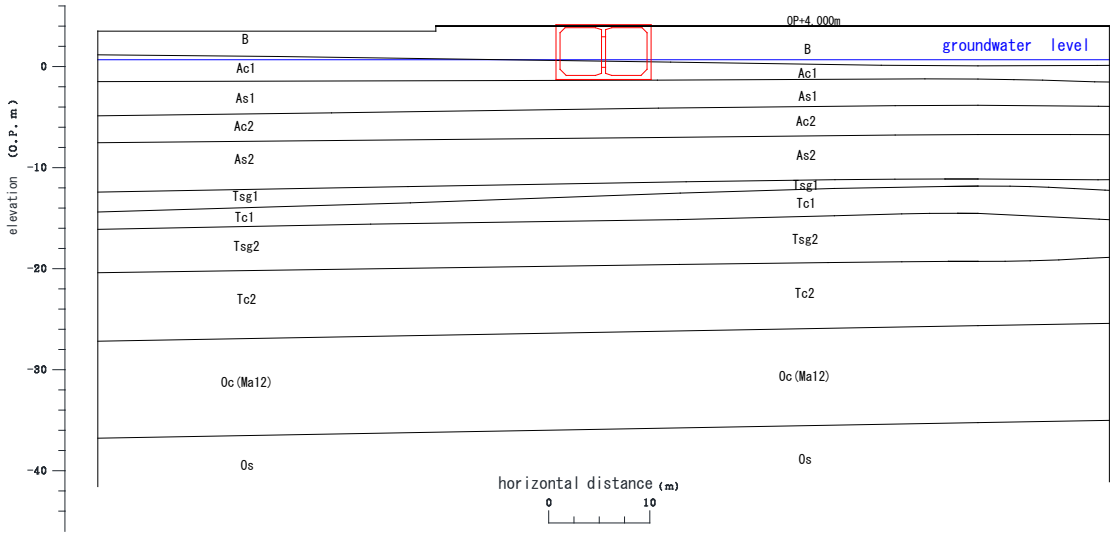

Fig. 1 Target ground of the analysis

Table 1 Material parameters used in analysis

	①		②	③	④	⑤	⑥	⑦	⑧	⑨
type	Bs Y	X	As1 X	Ac1, Ac2 Y	As2 X	Tsg1 Y	Tc1 Y	Tsg2 Y	Tc2 Y	Oc X
γ (kN/m^3)	18.0	18.0	18.0	16.0	18.0	16.0	18.0	16.0	16.0	18.0
ρ (g/cm^3)	1.8	1.8	1.8	1.6	1.8	1.6	1.8	1.6	1.6	1.8
k (m/s)	1.47 E-06	1.47 E-06	1.47 E-06	9.00 E-09	5.17 E-06	2.60 E-07	1.20 E-05	1.00 E-07	7.50 E-09	1.12 E-06
e_0	0.658	0.658	0.990	1.038	0.505	0.724	0.777	1.098	1.799	0.673
Vs (m/s)	120	140	120	120	240	200	260	208	208	170
λ		0.002	0.002		0.001					0.1
κ		0.025	0.02		0.001					0.02
OCR*		1.3	1.0		1.6					1
G_0/σ'_{m0}		935.5	445.3		1104					646.1
M^*_m		0.909	0.909		0.909					0.909
M^*_f		1.012	0.966		1.215					0.958
B^*_0		3500	2500		10000					5000
B^*_1		80	50		20					100
C_f		0	0		0					0
γ^{P*}_r		0.02	0.002		0.005					0.02
γ^{E*}_r		0.001	0.3		0.001					0.3
D^*_0		1.0	1.5		4.0					4
n		7.0	2.0		8.0					6
C_d		2000	2000		2000					2000
ν	0.496			0.496		0.494	0.488	0.492	0.492	
c (kPa)	0			33		198	0	149	149	
ϕ (deg)	30.9			0		0	34	0	0	
a	6977			2241		4939	8530	4533	4165	
b	0.5			0.5		0.5	0.5	0.5	0.5	
α	1.89			16.7		2.3	2	1.4	1.5	
r	1.92			1.78		2.1	3	1.7	1.6	

Notations:
X: cyclic elastoplastic constitutive model
Y: R-O model
γ = unit weight, ρ = density, k = coefficient of permeability, e_0 = initial void ratio, V_s = shear wave velocity, λ = compression index, κ = expansion index, M_f = stress ratio parameter corresponding to failure angle, OCR* = factoid overconsolidation ratio, G_0/σ'_{m0} = non-dimensional initial shear modulus, M_m = stress ratio parameter corresponding to phase transformation angle, B^*_0, B^*_1, and C_f = plastic modulus parameters, γ_r^{P*} = plastic strain, and γ_r^{E*} = elastic strain, D^*_0, n = dilatancy coefficient, C_d = anisotropy elimination parameter, ν = Poisson's ratio, c = cohesion, ϕ = internal friction angle, and a, b, α, and r = R-O parameters

2.2 Tunnel model

Figure 2 shows a model of the ground with the tunnel. The green lines indicate the tunnel. The tunnel consists of an upper base plate and a lower base plate, a sidewall, and a center pillar. The tunnel is represented by beam elements. Table 2 lists the tunnel parameters used in the analysis. B is the horizontal length of the element, and H is the vertical length of the element. The tunnel is made up of four kinds of boards. Those are base plate(upper), base plate(lower), side wall, center pillar.

We have confirmed that the tunnel will not be destroyed in this earthquake, so we do not consider destroying the tunnel.

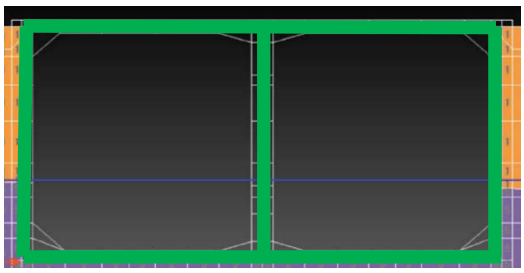

Fig. 2 Tunnel model

2.3 Boundary conditions

2.3.1 Soil skeleton

In the analysis model, the bottom of the boundary is an elastic base (viscous boundary). The elastic base is placed as a dashpot on the bottom of the model. The input earthquake motion is a 2E wave. In LIQCA, only the horizontal lower boundary can be set for the viscous boundary. When a consolidation analysis is conducted, the dashpot is automatically replaced with a rigid spring. The side boundary is a method of connecting a wide free ground part, which is not easily influenced by the FEM region, to the side surface when the soil layer configuration of the side boundary is different.

2.3.2 Tunnel

The boundary condition between the tunnel and adjacent ground is free from friction in the vertical direction. The tunnel and its adjacent ground behave similarly in the horizontal direction.

2.4 Input earthquake motion

The input earthquake motion is the seismic standard spectrum I, which is commonly used in Japan. The waveform is shown in Fig. 3. The increment of the calculation time is 0.005 s. The Newmark method coefficients are β = 0.3025 and γ = 0.6. These values are common in LIQCA simulations. The constant of the Rayleigh attenuation α_1 is equal to 0.001–0.003. The Rayleigh attenuation α_1 in the example of the LIQCA manual is 0.0023. After the seismic motion, consolidation analysis is carried out until the vertical settlement converges.

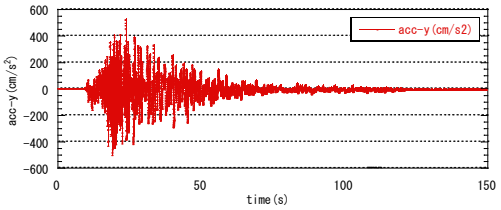

Fig. 3 Waveform of seismic standard spectrum I

Table 2 Tunnel parameters

	B (m)	H (m)	Pitch (m)	Unit volume weight γ(kN/m^3)	Sectional area A(m^2)	Sectional Secondary moment I(m^4)	Unit length Weight G(kN/m)
base plate (upper)	1	0.3	1	25	0.30	0.001125	7.5
base plate (lower)	1	0.4	1	25	0.40	0.002667	10
side wall	1	0.4	1	25	0.40	0.002667	10
center pillar	2.3	0.4	4	25	0.23	0.001533	5.75

2.5 Initial stress analysis

The initial values of the soil skeleton displacement and excess pore water pressure are all 0. The soil skeleton displacement and excess pore water pressure in LIQCA are the increments from the initial state, that is, the incremental values at the time of the earthquake. What is necessary under the initial conditions is to set the initial effective stress on the ground. Therefore, it is important to estimate the initial stress state on the ground. The initial stress analysis in this paper is a self-weight analysis. The self-weight analysis calculates the initial stress by applying self-weight to the model used for the liquefaction analysis in the zero-gravity state. It considers the increase in ground rigidity and nonlinearity caused by adding weight to the model.

3. ANALYSIS RESULT

The analysis results are shown below. After the earthquake motion, a consolidation analysis was carried out until the convergence of the vertical displacement was confirmed. The effective stress reduction ratio R is used as an index for determining liquefaction. It is shown by the following equation:

$$R = 1 - \frac{\sigma'_m}{\sigma'_{m0}} \quad (1)$$

σ'_m : average effective stress corresponding to some elapsed time (kN/m^2)

σ'_{m0} : average effective stress in the initial stress state (kN/m^2)

When this value reaches 1, it can be said that liquefaction occurred in the ground. The nodes and elements that output the analysis results are the vicinity of the tunnel center and the stratum of the point 25 m northward from the tunnel center.

3.1 At the stratum of the point 25 m northward from the tunnel center

Figure 4 shows the effective stress reduction ratio of As1, As2, and Tsg1. According to these results, it turns out that these soil layers become liquefied. The effective stress reduction ratio decreases after 10^8 s (approximately 3 years). This indicates that the excess pore water pressure that occurs by liquefaction is dissipated, and the consolidation settlement converged. Figures 5 and 6 show the vertical displacement and horizontal displacement, respectively. After the consolidation converges, the ground surface settles by 0.5 m in the vertical direction and moves 0.8 m in the horizontal direction.

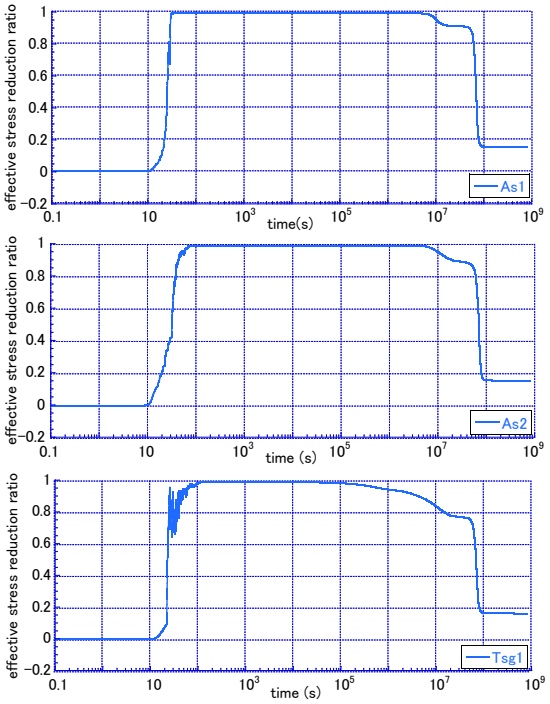

Fig. 4 Effective stress reduction ratio of As1, As2, and Tsg1 (25 m northward from tunnel center)

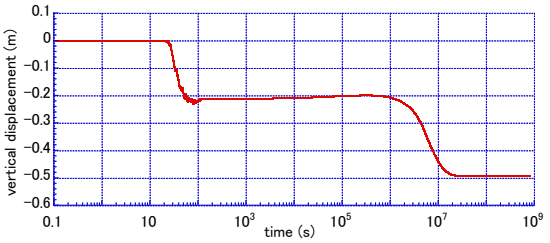

Fig. 5 Vertical displacement (25 m northward from tunnel center)

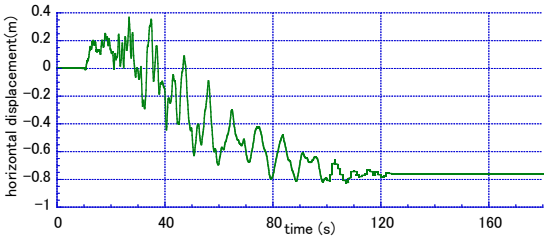

Fig. 6 Horizontal displacement (25 m northward from tunnel center)

3.3 In the vicinity of the tunnel center

Figure 7 shows the effective stress reduction ratio of As1, As2, and Tsg1. According to these results, it turns out that these soil layers become liquefied. Figures 8 and 9 show the vertical displacement and horizontal displacement, respectively. After the consolidation converges, the tunnel rises by 0.9 cm in the vertical direction and moves 0.8 cm in the horizontal direction.

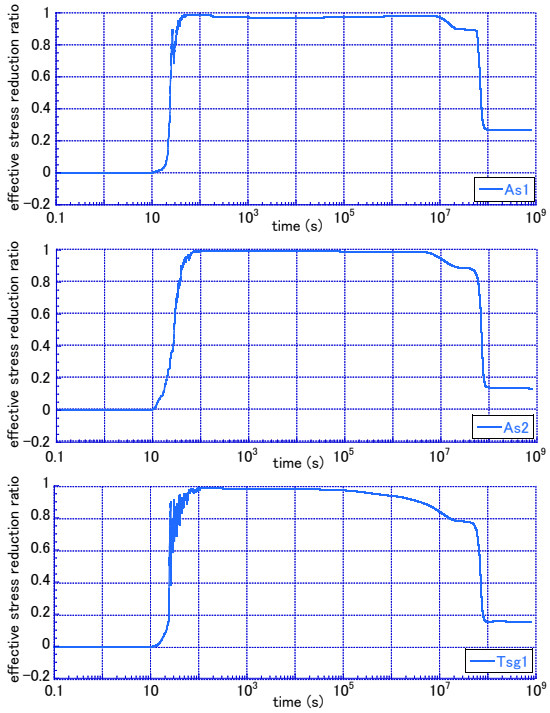

Fig. 7 Effective stress reduction ratio of As1, As2, and Tsg1 (tunnel center)

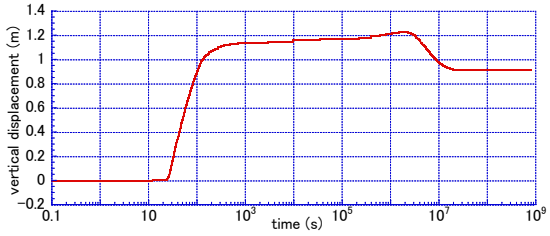

Fig. 8 Vertical displacement (tunnel center)

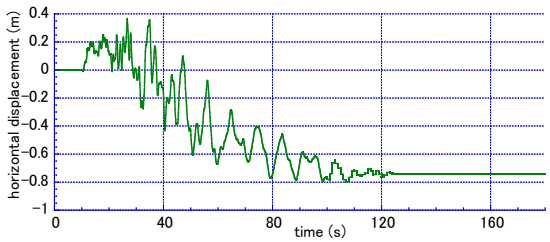

Fig. 9 Horizontal displacement (tunnel center)

3.4 Summary of some indices

Table 3 lists the results of the effective stress reduction ratio (just after excitation). Table 4 lists the results of the effective stress reduction ratio (after consolidation). Point A corresponds to the stratum, which is 25 m northward from the tunnel center. Point B corresponds to the vicinity of the tunnel center.

Table 3 Effective stress reduction ratio (after excitation)

	Effective stress reduction ratio (%)		
	As1	As2	Tsg1
A	99.9	99.9	99.9
B	99.9	99.9	99.9

Table 4 Effective stress reduction ratio (after consolidation)

	A	B
horizontal displacement (m)	−0.733	−0.758
Vertical displacement (m)	0.898	−0.496

3.5 Displacement of the ground surface

Figure 10 shows the vertical displacement for each time history. The data corresponds to the state of the initial coordinate after excitation and after the consolidation of the ground surface coordinates. The part from 45 to 55 m of the X coordinate is the tunnel position. When the state after consolidation is examined, it can be seen that the tunnel rises by 0.9 m. This phenomenon is caused by the boundary condition between the side surface of the tunnel and the surrounding ground. The boundary was set under a free condition in the vertical direction, which has no friction. Therefore, a settlement of 0.9 m is thought to be the maximum floating amount.
In this analysis, we do not consider the changes in the buoyancy of the surroundings owing to the floating of the tunnel. In other words, the buoyancy around the tunnel remains in its initial state. In addition, this is considered to be a cause of the large level of floating of the tunnel. The other surface part, except for the tunnel position, settles at approximately 50 cm after consolidation.

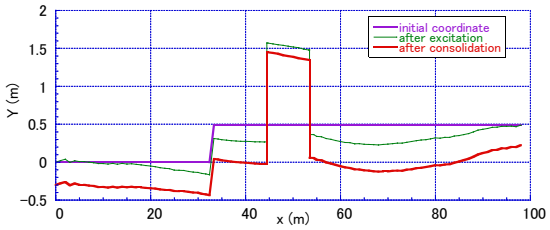

Fig. 10 Vertical displacement for each time history

3.6 Deformation map of the ground

Figure 11 shows the deformation of the ground around the tunnel after consolidation. The floating of the tunnel may depend on how the sediment cuts under the tunnel when the As1 layer around the tunnel becomes liquefied. The floating of the tunnel is approximately 0.9 m. However, this value is perhaps the maximum floating amount, as mentioned earlier. In fact, there is friction between

the tunnel and the surrounding ground, so it is highly likely that the floating of the tunnel may have a smaller value than that of the analysis result.

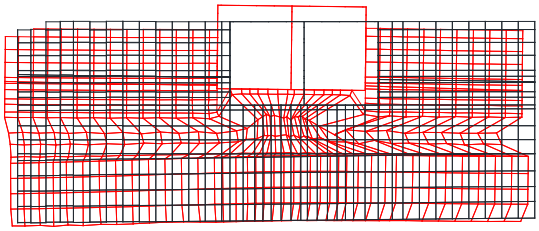

Fig. 11 Deformation around the tunnel

4. CONCLUSION

When an earthquake corresponding to seismic standard spectrum I occur at the target ground of the Osaka Gulf coast, from the results of a liquefaction simulation based on LIQCA, it turns out that the ground becomes liquefied and the tunnel at the surface of the target ground floats up slightly. It is necessary to investigate the floating amount more precisely, hereafter, because the floating has a serious impact on the restoration process of the target area.

However, a settlement of 0.9 m is thought to be the maximum value of the floating amount. This phenomenon is caused by the boundary condition between the tunnel and the surrounding ground. In addition, we did not consider the changes in the buoyancy of the surrounding ground. We think that it is necessary to make this phenomenon more realistic. The buoyancy problem may be difficult. Therefore, we will further investigate the boundary condition between the sidewall of the tunnel and the adjacent ground. We will conduct more realistic simulations.

5. REFERENCES

[1] Matsuoka S, Wakamatsu K, and Hashimoto K, “Estimation method of liquefaction risk based on topography: Ground classification 250 m mesh map”, in Proc. of the Japan Earthquake Engineering Association, 2011, pp. 35–36.

[2] LIQCA Liquefaction Geo-Research Institute: LIQCA 2 D 15 · LIQCA 3 D 15 material, 2015.

[3] Railway Technical Research Institute, Design Standards for Railway Structures and Commentary, 2012.

[4] Yasuda S, and Yamaguchi I, “Dynamic deformation characteristics of various undisturbed soils”, of the 20th Soil Engineering Research Presentation, 1985, pp. 539–542.